NUCLEAR SCIENCE AND ENGINEERING: **134**, 50–67 (2000)

Neutron Capture and Total Cross-Section Measurements and Resonance Parameter Analysis of Zirconium up to 2.5 keV

G. Leinweber,* J. Burke, C. R. Lubitz, H. D. Knox, and N. J. Drindak

Lockheed Martin Corporation, P.O. Box 1072, Schenectady, New York 12301-1072

and

R. C. Block, R. E. Slovacek, C. J. Werner,† N. C. Francis, Y. Danon,‡ and B. E. Moretti§

Rensselaer Polytechnic Institute, Environmental and Energy Engineering Department
Troy, New York 12180-3590

Received August 28, 1998
Accepted April 8, 1999

Abstract—*Neutron capture and transmission measurements were performed by the time-of-flight technique at the Rensselaer Polytechnic Institute LINAC using metallic zirconium samples. The capture measurement was made at the 25-m flight station with a multiplicity-type capture detector, and the transmission total cross-section measurements were performed at the 25-m flight station with a ^{6}Li glass scintillation detector. Resonance parameters were determined by a combined analysis of all 11 data sets (4 capture and 7 transmission) using the least-squares multilevel R-matrix code REFIT.*

The present measurements were undertaken to resolve discrepancies between common usage (ENDF/B-VI) and the recent measurements of Salah et al. for the 300-eV zirconium doublet. The present measurements support the Salah et al. conclusions. Specifically, the results confirm the assignment of $J = 3$ for the ^{91}Zr 292.5-eV resonance and include all significant resonances up to 2.5 keV. The zirconium resonance parameters Γ_γ and Γ_n, determined in the present measurement, are compared with the ENDF/B-VI parameters.

I. INTRODUCTION

For many years, the accuracy of measured cross sections exceeded the precision of the computer codes used for nuclear reactor calculations. With the increased use of Monte Carlo methods utilizing increased computer memory for more detailed models and greater speed to permit more histories, this situation changed. The accuracy of many current Monte Carlo calculations is now limited by the accuracy of the cross-section data being used.

To improve the accuracy of the measured data, the Rensselaer Polytechnic Institute (RPI) Cross-Section Group has been actively upgrading the experimental equipment used in the measurement program at the RPI LINAC facility. A high-efficiency 16-segment multiplicity-type gamma detector was developed for use in neutron capture measurements.[1–3] An improved time-of-flight (TOF) analyzer that interfaces directly to a data-taking computer was designed and constructed to handle high-accuracy and high-count-rate measurements. Improved LINAC targets were developed to provide enhanced neutron production in the few electronvolt range, where contributions to the resonance integral are greatest. Special-purpose data reduction software has been written to manipulate the data arrays, and state-of-the-art

*E-mail: leinwg@rpi.edu

†Current address: Los Alamos National Laboratory, Los Alamos, New Mexico 87545.

‡Current address: Nuclear Research Center, Negev, P.O. Box 9001, Beer-Sheeva, Israel.

§Current address: United States Military Academy, West Point, New York 10996.

analysis software[4] was obtained, thanks to M. C. Moxon, from the Harwell Laboratory for neutron resonance parameter extraction. Recent work at RPI using the upgraded equipment is given by Danon et al.[5] for rare earth elements and by Werner[6] for tungsten.

Table I provides a historical summary of zirconium measurements of the 300-eV doublet. Many previous measurements used samples enriched in ^{91}Zr and determined parameters for the 292.5-eV resonance only. The spin assignment for this resonance has a conflicting history, as Table I shows. The most recent work is that of Salah et al.[8] who found this to be an s-wave resonance with $J = 3$. The historical work on the 301.1-eV p-wave resonance in ^{96}Zr was less extensive. Here J is defined as the total angular momentum. An s-wave resonance has an orbital angular momentum $l = 0$. A p-wave resonance has an orbital angular momentum $l = 1$. All references agreed that the 292.5-eV resonance is an s-wave and the 301.1-eV resonance is a p-wave.

II. EXPERIMENTAL CONDITIONS

Neutrons are generated via photoneutron reactions caused by the ~54 MeV pulsed electron beam from the RPI LINAC. The pulse of electrons strikes a water-cooled tantalum target, where electrons generate bremsstrahlung, which in turn produces photoneutrons. The neutrons are then moderated and collimated as they drift down a long flight tube to the sample and detector.

The present RPI zirconium data were obtained from three measurements of zirconium performed at the RPI LINAC facility. Two were neutron transmission measurements, and one was neutron capture. The LINAC target used for all three experiments was the traditional "bounce" target,[19] where the tantalum plates are mounted off the neutron beam axis, and a 1-in.-thick polyethylene moderator is mounted adjacent to them and centered on the neutron beam axis. Neutrons are slowed by and emitted from the moderator and then drift down the flight tube to the detector.

The neutron energy for a detected event is determined using the TOF technique. The time from the LINAC electron burst, which creates the neutrons, to the time of the detected event is used to determine the flight time of the neutron. Combining this with precise knowledge of the flight path length gives the neutron energy. The TOF analyzer[1] used in these experiments was designed and constructed in-house and incorporates a 32-MHz crystal-controlled oscillator coupled to a high-speed scaler with 22-bit resolution. It operates as a single-start/multiple-stop device; i.e., a single LINAC burst initiates a countdown cycle, during which any number of detected events cause the analyzer to record an event. The TOF analyzer employs a fixed dead time of 0.250 μs to record each event.[1,19] The overall dead time of the signal processing electronics was set at 1.125 μs for capture measurements and at 0.6 μs for transmission measurements.[20] The entire data-taking process was controlled by a Hewlett-Packard HP-1000 model A990 computer. During operation of the experiment, data are transferred from the TOF analyzer to the computer memory via direct memory access. The data-taking software is completely menu driven and controls the sample changer, sorts the data into individual spectra, and provides on-line display of the data being accumulated. A description of the TOF analyzer, data-taking computer system, data file structure, and data reduction process is provided in Ref. 1.

II.A. Capture Detector

The capture detector is a multiplicity-type scintillation gamma detector containing 16 optically isolated sections of NaI(Tl), formed into a 30.5- × 30.5-cm (12- × 12-in.) right circular cylinder with an 8.9-cm (3.5-in.) through hole along its axis.[1–3] The cylinder is split across its axis into two rings, with each ring divided into eight equal pie-shaped segments. Each segment is hermetically sealed in an aluminum can and is viewed by an RCA 8575 photomultiplier tube. The total volume of NaI(Tl) is 20 ℓ. The capture detector used for the present measurements was located at the east beam tube at a flight path of 25.570 ± 0.003 m from the bounce target.[19] The flight path length was determined from measurements of precisely known ^{238}U resonances.

The efficiency of the multiplicity detector varies with the number and energy of gammas emitted in a capture event. A single particle model distribution of capture gammas in various zirconium isotopes has been coupled to a Monte Carlo simulation of the transport of various gamma cascades from the central sample location into the detector segments. This method is described in Ref. 21. Over the range of multiplicities that have been measured at RPI, this calculation has shown a direct proportionality between measured multiplicity and efficiency. Detector efficiency, calculated with this method, is 58% for a single 2-MeV gamma ray. The average multiplicity measured in ^{91}Zr resonances is ~4.3, which results in 95% efficiency. The average multiplicity measured in the 301-eV resonance in ^{96}Zr is 2.2, which results in 87% efficiency. Therefore, within the resonance parameter fitting process, the reduction in efficiency for ^{96}Zr capture compared with ^{91}Zr was incorporated into all results reported here. The capture detector efficiency of all other isotopes was assumed to be the same as that of ^{91}Zr.

Samples 5 cm in diameter are precisely positioned at the center of the detector by a computer-controlled sample changer. The sample changer accommodates up to eight samples and moves them into the beam one at a time. Neutrons that scatter from the sample are absorbed by a hollow cylindrical liner fabricated of boron carbide ceramic to reduce the number of scattered neutrons reaching the detector. The liner uses boron enriched to 99.4 wt% ^{10}B for maximum neutron absorption. A

15-cm (6-in.)-thick, 7260-kg (16 000-lb) lead shield surrounds the detector to reduce the gamma-ray background. Reference 1 contains a description of the detector and its signal processing electronics.

II.B. Transmission Detector

The transmission detector was a 12.70-cm (5-in.)-diam, 1.27-cm-thick NE 905 ^{6}Li glass detector (6.6% lithium, enriched to 95% in ^{6}Li). This was the optimum thickness for the 10- to 500-eV neutron energy range. The detector was coupled to a photomultiplier tube, which was in line with the flight path. The transmission detector used was located at the center beam tube at a flight path of 25.5815 ± 0.0030 m from the bounce target.[19] This flight path length was traceable to measurements of precisely known ^{238}U resonances.[22]

Transmission samples along with two empty sample holders, which are used to measure the open beam count rate, were mounted on an eight-position computer-controlled sample changer. The transmission function, which is the ratio of the count rate with a sample in the beam to the count rate with samples removed, varies with neutron energy. Each run consisted of one or more complete cycles through the samples, with a predetermined number of LINAC electron pulses for each sample position. The distribution of electron pulses per sample position was chosen to minimize the counting statistical error in the transmission.

III. DATA REDUCTION

III.A. Capture Data

A capture experiment typically involved taking several types of data. Sample data were taken with up to eight samples mounted on the sample changer. These usually included four samples of different thickness, a sample for flux normalization, and two or three empty sample holders for background evaluation. Thirty-two TOF spectra with 8192 channels each were measured for each sample, i.e., 16 spectra of capture data and 16 spectra of scattering data, which gave a data file size of 8 MB per run. A minimum of 100-keV gamma energy was required in a detector segment to be counted. Data were recorded as capture events if the total energy deposited in all 16 detector segments exceeded 1 MeV. Data were recorded as scattering events if the total gamma energy deposited fell between 360 and 600 keV. In this energy region lies the 478-keV gamma emitted following an (n,α) reaction in the $^{10}B_4C$ annular detector liner. Capture gamma-ray multiplicity data were also taken and used to estimate the detector efficiency decrement for ^{96}Zr + n cascades relative to other zirconium isotopes.

TABLE

A Historical Survey of Zirconium Resonance

Experimenters + Reference Numbers	Year	Laboratory	Types of Experiments	Samples Used
Present measurements	1998	RPI	Trans + capture	Zr-nat
ENDF/B-VI[7]	1997	Brookhaven	Evaluation only	No experiment
Salah et al.[8]	1985	Oak Ridge	Trans only	4 Zr-nat + 1 Zircaloy
Mughabghab, Divadeenam, and Holden[9]	1981	Brookhaven	Evaluation only	No experiment
Brusegan et al.[10]	1978	Geel	Trans + capture + gamma spectra	89.2% $^{91}ZrO_2$ + Zr-nat
Musgrove et al.[11]	1977	Oak Ridge	Trans + capture	89.2% ^{91}Zr for trans 0.5 mm 88.6% ^{91}Zr for cap
Macklin et al.[12]	1977	Oak Ridge	Trans + capture	Zr-nat 3 mm for cap
Mughabghab and Garber[13]	1973	Brookhaven	Evaluation only	No experiment
Rimawi[14]	1969	SUNY Albany	Gamma spectra with GeLi	Zircaloy
Bartolome et al.[15]	1969	RPI	Trans + capture	Various ZrO_2, enriched in ^{90}Zr, ^{91}Zr, ^{92}Zr, or ^{94}Zr
Morgenstern et al.[16]	1969	Saclay	Trans only	Zr-nat
Lopez et al.[17]	1968	Gulf General Atomic	Trans, capture + self-indication	5 Zr-nat + 91% ^{91}Zr + 89% ^{91}Zr
BNL-325[18]	1966	Brookhaven	Evaluation only	No experiment

[a]Salah et al.[8] quotes Coceva's reanalysis of Ref. 10 and 11 data to $\Gamma_n = 634 \pm 17$ meV.
[b]Average over all ^{91}Zr s-wave resonances.

The LINAC electron pulse width for the zirconium capture measurement was 100 ns, and the channel width at 300 eV was 125 ns with an average accelerator current of ~35 μA. The data-taking session lasted 70 h at 200 pulses/s. To minimize data loss in the event of an equipment malfunction and to average out LINAC beam intensity fluctuations, an individual run duration of ~1 h was used. Multiple runs were summed off line to accumulate the necessary statistical accuracy.

Once accumulated, the TOF data were subjected to a "consistency check" in which data were only accepted when the recorded detector counts and beam monitor counts fell within a range of statistical fluctuations. Any data where malfunctions occurred were eliminated. Next, all data were dead-time corrected, similar data sets were combined into composite data runs, and the runs were normalized to the neutron beam fluence using fixed monitor detectors on the same and alternate beam tubes. Background was determined using normalized data measured with an empty sample holder mounted in the sample changer. Background spectra evaluated in this manner were subtracted from the normalized, summed spectra. Finally, the 16 individual multiplicity spectra were collapsed into a single combined total spectrum.

In addition to the sample data, another set of data was needed to determine the neutron beam's flux profile. This was done by mounting a thick $^{10}B_4C$ sample in the sample changer and adjusting the threshold to record the 478-keV gamma rays from neutron absorption. Because the sample used is black up to 300 eV, the maximum energy at which capture data were used, the boron absorption spectrum provided an accurate representation of the LINAC's neutron beam flux profile. These flux data gave the shape of the neutron beam flux, but not its magnitude. To convert it to a flux profile normalized to the same fluence as the capture sample data, the flux shape was normalized to the black 4.9-eV resonance in gold, which was included among the capture samples. The flux was further normalized by an erbium/gold factor of 1.15 determined at RPI to account for the hard spectrum of capture gamma rays and scattering effects from gold, which result in an uncharacteristically low detector efficiency.

The zero time for capture was determined for the capture experiment by limiting the number of active detector segments and measuring a partially attenuated gamma flash from the electron target. Finally, the capture yield (the fraction of incident neutrons that undergo capture) for each sample was produced by dividing its normalized and corrected capture spectrum (summed over all 16 multiplicities) by the normalized neutron flux spectrum. It was this capture yield that provided input to the REFIT data analysis code[4] that extracted the neutron resonance parameters.

I

Parameters, Measurements, and Publications

	292 eV			301 eV		
J	E (eV)	Γ_γ (meV)	Γ_n (meV)	E (eV)	Γ_γ (meV)	Γ_n (meV)
3	292.5 ± 0.1	125.9 ± 2.1	645.0 ± 2.2	301.1 ± 0.1	143.3 ± 7.0	221.6 ± 2.7
2	292.6	100	864	301.0	258	215.0
3	292.40 ± 0.10	131 ± 10	665 ± 5	301.14 ± 0.10	285 ± 38	223 ± 7
2	292.6 ± 0.3	100 ± 20	864 ± 11	301.0 ± 0.3	258 ± 15	215 ± 2.5
3	292.41	121 ± 14	612 ± 6[a]			
2	292.7	140 ± 8[b]	766 ± 20[a]			
2	292.36	86.8 ± 2.2	866 ± 11			
2	292.0 ± 0.3	150 ± 30	762 ± 48	302 ± 1	250 ± 20	190 ± 30
2						
3		180 ± 30	570 ± 70			
3	292.37	100 ± 50	670 ± 30			
3	292	120 ± 30	635 ± 40			
3	293 ± 1	190 ± 100	575 ± 60	302 ± 1	250 ± 60	190 ± 30

Table II lists the number densities for the four capture samples used in the present measurements. Capture samples were natural metal zirconium 0.051, 0.10, 0.20, and 0.51 mm (nominal) thick (0.002, 0.004, 0.008, and 0.020 in. thick). Data from the two thickest samples were only used for weakly scattering resonances where multiple scattering is not significant. All samples listed were natural zirconium metal mounted inside aluminum sample holders with the front and back faces cut away. Only a very small lip of aluminum remained in the periphery of the beam to secure the sample. The effect of these sample holders was removed by including an empty sample holder in the background measurement.

III.B. Transmission Data

The LINAC electron pulse width was 40 ns, and the channel width at 300 eV was 125 ns for the first of two transmission measurements. The average accelerator current was ~28 μA, and the experiment ran for 70 h at 310 pulses/s.

The LINAC electron pulse width was 40 ns, and the channel width at 300 eV was 31.25 ns for the second transmission measurement. The average accelerator current was ~38 μA, and the experiment ran for 46 h at 310 pulses/s.

As with capture measurements, a transmission measurement consisted of many individual runs of ~1-h duration, which were summed off line to provide the necessary statistical accuracy. Normally, two sample positions were used to measure open beam count rate, and these were placed at the beginning and middle of each sample cycle. The time split between samples and open beam was optimized to reduce the counting statistics error.

The large amount of data collected in each experiment was first run through a statistical consistency check, as discussed earlier for capture, to verify the stability of the LINAC, the in-beam detector, and the beam monitors. The data were then corrected for dead time, and the runs were normalized and summed. Time-dependent background was obtained with the one-notch/two-notch method.[23] This method employs blacked-out notch filters of single and double material thickness, and the resulting background determined from each is extrapolated back to zero effective material thickness. The measured background was then fitted to a smooth analytical function of TOF for each sample, including the open beam measurement. The resulting analytical expression was used for the background correction. Finally, T_i, the transmission in TOF channel i, was calculated as follows:

$$T_i = \frac{(C_i^s - K_s B_i - B_s)}{(C_i^o - K_o B_i - B_o)} \quad , \tag{1}$$

where

C_i^s, C_i^o = dead-time corrected and normalized counting rates of the sample and open measurements, respectively

B_i = unnormalized time-dependent background counting rate

B_s, B_o = steady-state background counting rates for sample and open measurements, respectively

K_s, K_o = normalization factors for the sample and open measurements.

The normalization factors K_s and K_o were determined by forcing the smooth analytical background function through a particular notch-extrapolated background point. Had a saturated resonance been present in the sample, it, rather than the notch-extrapolated background point, would have been used to calculate K_s.

The zero time for the transmission experiments was determined from fitting well-known resonances in uranium for the three ^{238}U samples, which were among the transmission samples measured in the first transmission experiment.

Table III lists the number densities for the seven transmission samples used in these measurements. Transmission samples were natural zirconium 0.56, 1.8, 2.5, 5.1, 7.6, and 10 mm (0.022, 0.070, 0.100, 0.200, 0.300, and 0.400 in.) thick.

TABLE II

Zirconium Capture Samples*

Nominal Thickness		Number Density (atom/b)
(mm)	(in.)	
0.051	0.002	0.00021711 (0.00000004)
0.10	0.004	0.00042399 (0.00000007)
0.20	0.008	0.00089419 (0.00000013)
0.51	0.020	0.00228236 (0.00000049)

*Uncertainties (1σ) in parentheses.

IV. METHODS

Resonance parameters were extracted from the capture and transmission data sets using the least-squares multilevel *R*-matrix code REFIT (Ref. 4). The free gas Doppler broadening model, with an effective temperature of 300 K, was used in the REFIT calculations.

REFIT describes resolution broadening in terms of physically meaningful components: electron pulse width, decay time in the neutron producing target, time delay in the moderator, TOF channel width, and detector resolution function. For capture measurements, the detector was

TABLE III

Zirconium Transmission Samples*

Nominal Thickness		Number Density (atom/b)
(mm)	(in.)	
10	0.400	0.0427827 (0.0000231)
7.6[a]	0.300[a]	0.0333194 (0.0000044)[a]
7.6[b]	0.300[b]	0.0334886 (0.0000046)[b]
5.1	0.200	0.0214950 (0.0000031)
2.5	0.100	0.0118245 (0.0000032)
1.8	0.070	0.0078736 (0.0000010)
0.56	0.022	0.0024221 (0.0000002)

*Uncertainties (1σ) in parentheses.
[a]Used in the first of two transmission experiments.
[b]Used in the second of two transmission experiments.

not in line with the neutron beam, so there is no detector resolution broadening. The LINAC and target-dependent components are described as a primary pulse with a target decay time and a smaller secondary pulse with a specific amplitude and tail in time. The resolution parameters used to analyze the zirconium data were derived specifically for the RPI LINAC facility in its present configuration.

For the transmission measurements, where the detector was in line with the neutron beam, a detector resolution function was included in the analysis. The REFIT user's manual[4] does not provide an explicit functional form for the ^{6}Li detector resolution function. Rather, it is described by the REFIT input parameters listed in Table IV. These transmission detector resolution parameters were recommended by the REFIT code's author based on his experience with detector systems similar to the present RPI LINAC facility configuration.

TABLE IV

Input Parameters for REFIT's Detector Resolution Function

Component	Value
Detector type	Slab
Detector length in neutron beam	0.003 m
Detector diameter	0.0508 m
Thickness for scattering	0.024 atom/b
Thickness for reaction	0.003 atom/b
Scattering cross section of detector	2.4 b
Reaction cross section of detector	$140E^{-0.5}$ b; E = neutron energy (eV)
Multiplying factor for scattering correction	3.0
Multiplying factor for mean free path	3.0

Self-shielding and multiple scattering corrections were applied in REFIT for all capture analyses. Thick sample data were used only when a resonance had a small scatter-to-capture ratio and a poor signal-to-background ratio in thinner sample data.

The capture detector efficiency for the ^{96}Zr + n cascades (capture in 301-eV resonance) was calculated to be 8% below all other zirconium isotopes. This decrement was identified from a lower average measured multiplicity and is attributed to a hard spectrum (fewer gammas) and a low neutron separation energy (less energy available to detect). The effect was quantified using a method of single-particle-model-generated gamma cascades coupled to Monte Carlo transport within the detector system geometry.[21] The effect was implemented in the mechanical operation of REFIT for capture fits by creating an effective abundance of the ^{96}Zr isotope 8% lower than the actual value.

The fitting procedure used an initial set of resonance parameters from ENDF/B-VI (Ref. 7) as a starting point. As recommended in the REFIT user's manual, normalization was fit to transmission data, and background was fit to capture data. Fits on limited energy regions were made to fit resonance energies and widths Γ_γ and Γ_n. A final combined analysis over the entire 100- to 2500-eV energy range using the regionally fit parameter results as initial values was then performed. This final fit ensured consistency among all analyzed resonances.

The channel radius used was 7.42 fm (Ref. 7), and no external R-function was employed. The calculation fitted the resonance energy E_0 and the resonance widths Γ_γ and Γ_n. In some cases, particularly at higher energies, the data were not sufficient to permit a reliable fit to Γ_γ. In those cases, Γ_γ was set to the ENDF/B-VI value, and only Γ_n was fit. This occurred for resonances at 681, 2240, and 2474 eV. For the strong scattering resonances at 182 and 240 eV, fits were performed with and without Γ_γ as a variable. Although the fit is fairly insensitive to the choice of Γ_γ in these resonances, the best fit values are presented.

Capture resonance integrals from 0.5 eV to 20 MeV and thermal capture cross sections were calculated for both ^{91}Zr and elemental zirconium using ENDF/B-VI parameters for all resonances. Capture resonance integrals and thermal capture cross sections were then recalculated substituting the current set of resonance parameters for the ENDF/B-VI values.

V. RESULTS

The results of the fitting process for all resolved resonances up to 2.5 keV are given in Table V. The results of the present measurements are compared with the ENDF/B-VI evaluation. For the zirconium resonances presented here, the ENDF parameters are identical to those

TABLE V

Zirconium Resonance Parameters*

Isotope	Resonance Parameters	ENDF/B-VI[7] (Mughabghab, Divadeenam, and Holden[9] Uncertainties)[a]	Present Measurements	Samples Transmission / Samples Capture	Other Experiments
^{91}Zr (abun = 11%)	Energy (eV) *l*, *J*	181.7 (0.2) 1, 3	181.9 (0.1) 1, 4	All 7 samples	Brusegan et al.[10] Musgrove et al.[11] Bartolome et al.[15] Lopez et al.[17]
	Γ_γ (meV) Γ_n (meV)	180 (18) 8.61 (0.34)	275 (16) 6.41 (0.08)	All 4 samples	
^{91}Zr (abun = 11%)	Energy (eV) *l*, *J*	240.1 (0.2) 1, 2	240.3 (0.1) 1, 2	10 mm only	Brusegan et al.[10] Musgrove et al.[11] Bartolome et al.[15] Lopez et al.[17]
	Γ_γ (meV) Γ_n (meV)	270 (50) 4.32 (0.24)	143 (12) 3.52 (0.12)	0.10, 0.20, 0.51 mm	
^{91}Zr (abun = 11%)	Energy (eV) *l*, *J*	292.6 (0.3) 0, 2	292.5 (0.1) 0, 3	All 7 samples	See Table I
	Γ_γ (meV) Γ_n (meV)	100 (20) 864 (11)	125.9 (2.1) 645.0 (2.2)	0.051, 0.10 mm	
^{96}Zr (abun = 2.8%)	Energy (eV) *l*, *J*	301.0 (0.3) 1, 0.5	301.1 (0.1) 1, 0.5	All 7 samples	See Table I
	Γ_γ (meV) Γ_n (meV)	258 (15) 215.0 (2.5)	143.3 (7.0) 221.6 (2.7)	0.051, 0.10 mm	
^{91}Zr (abun = 11%)	Energy (eV) *l*, *J*	681.4 (0.7) 0, 3	681.4 (0.1) 0, 3	All 7 samples	Brusegan et al.[10] Musgrove et al.[11] Bartolome et al.[15] Lopez et al.[17]
	Γ_γ (meV) Γ_n (meV)	122 (15) 823 (20)	122 922 (8)	None	
^{94}Zr (abun = 17.38%)	Energy (eV) *l*, *J*	2243 (3) 0, 0.5	2239 (1) 0, 0.5	All except 0.56 mm	Not applicable
	Γ_γ (meV) Γ_n (meV)	97 (10) 1230 (50)	97 1707 (35)	None	
^{91}Zr (abun = 11%)	Energy (eV) *l*, *J*	2361.2 (2.0) 0, 3	Not observed	All except 0.56 mm	Brusegan et al.[10] Musgrove et al.[11] Bartolome et al.[15b]
	Γ_γ (meV) Γ_n (meV)	136 3514 (600)		None	
^{91}Zr (Abun = 11%)	Energy (eV) *l*, *J*	2383.3 (2.4) 1, 3	Not observed	All except 0.56 mm	Brusegan et al.[10] Musgrove et al.[11] Bartolome et al.[15b] Lopez et al.[17]
	Γ_γ (meV) Γ_n (meV)	252 (30) 146 (13)		None	
^{91}Zr (abun = 11%)	Energy (eV) *l*, *J*	2474.2 (2.5) 0, 2	2474 (1) 0, 2	All except 0.56 mm	Brusegan et al.[10] Musgrove et al.[11] Bartolome et al.[15] Lopez et al.[17]
	Γ_γ (meV) Γ_n (meV)	140 (20) 5784 (192)	140 6284 (107)	None	

*Uncertainties (1σ) in parentheses. The quoted uncertainties in the parameters from the present measurements reflect only the propagated counting statistics from the data.

[a]The ENDF database does not include uncertainties. Mughabghab, Divadeenam, and Holden[9] uncertainties are included to serve as a guide to the accuracy of these parameters.

[b]Observed one of two resonances, at $E_0 = 2373$ eV.

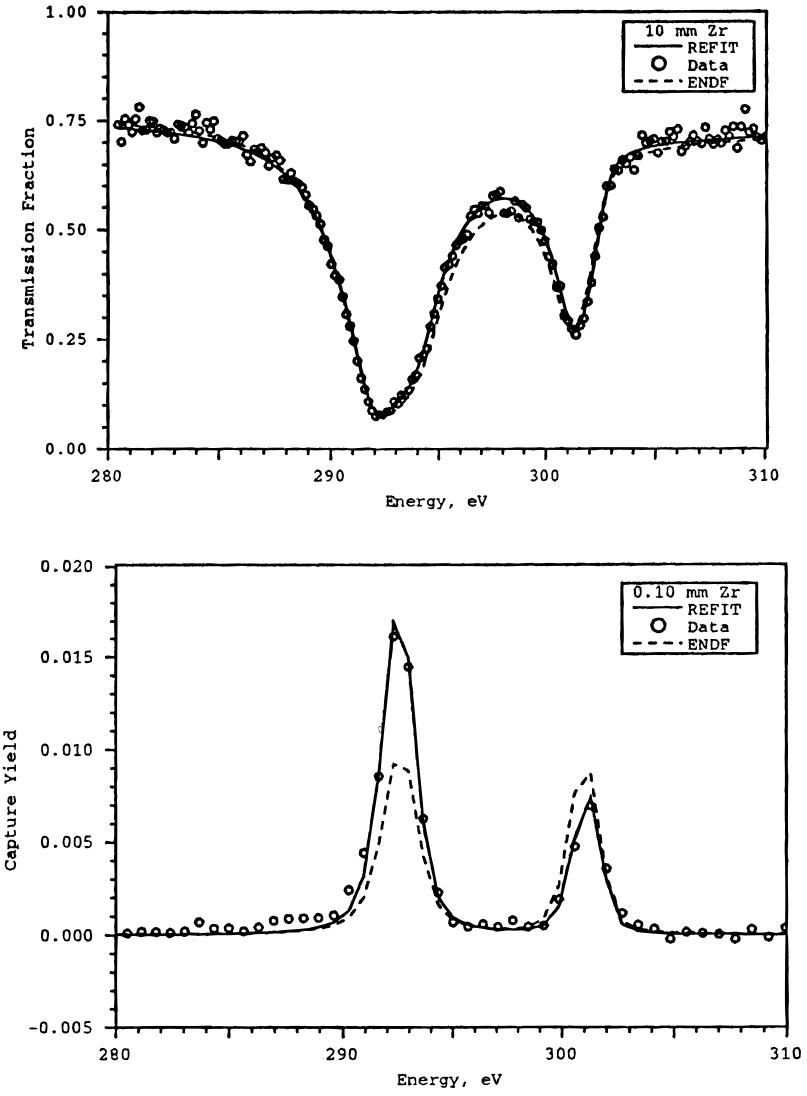

	ENDF J=2	Present Measurements J=3	ENDF J=½	Present Measurements J=½
Energy, (eV)	292.6	292.5 +/- 0.1	301.0	301.1 +/- 0.1
Γ_γ (meV)	100	125.9 +/- 2.1	258	143.3 +/- 7.0
Γ_n (meV)	864	645.0 +/- 2.2	215.0	221.6 +/- 2.7

Fig. 1. 292-eV s-wave resonance in ^{91}Zr 301-eV p-wave resonance in ^{96}Zr.

of Mughabghab, Divadeenam, and Holden,[9] whose uncertainties are quoted. The samples used to analyze each resonance are shown in Table V. Also, references to prior experiments for each resonance are given in the rightmost column of Table V.

Examples comparing the results of the fit using these parameters with typical measured spectra are shown in Figs. 1 through 6. Note that the REFIT curves represent the results combining all the data listed in Table V, whereas the data shown are only one particular data set. Details of the data sets are given in Tables II and III.

Figure 1 shows the final results for the 300-eV doublet. The figure includes resonance energy, isotope and spin assignment, a sample transmission and capture data

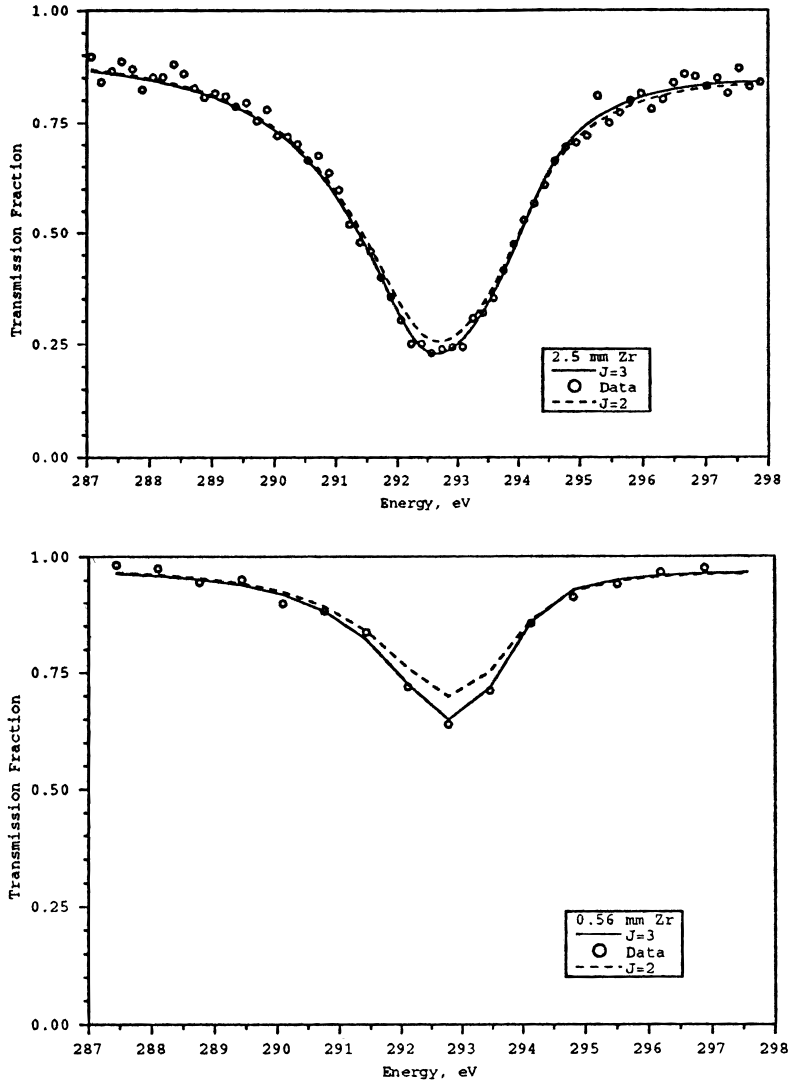

	Best Fit with J=2	Best Fit with J=3
Energy, (eV)	292.6	292.6
Γ_γ (meV)	182.9 +/- 3.3	125.9 +/- 2.1
Γ_n (meV)	779.4 +/- 2.7	645.0 +/- 2.2

Fig. 2. 292-eV s-wave resonance in ^{91}Zr; $J = 3$ versus $J = 2$.

set plotted with a calculated curve formed from ENDF, and the present measurement's resonance parameters, Doppler and resolution broadened. The resonance parameters corresponding to the calculated curves are shown in the table below the figure. A spin assignment of $J = 3$ has been deduced from the data for the 292-eV resonance. Best fit calculations for $J = 3$ and $J = 2$ are shown in Fig. 2 along with their corresponding resonance parameters.

Figure 3 shows the 182-eV p-wave resonance in ^{91}Zr. Figure 4 presents results from the 240-eV p-wave resonance in ^{91}Zr. As shown from the transmission plot, this resonance is weak. Therefore, only the thickest (10 mm) transmission sample data are used in the fit.

Results from the 681-eV s-wave resonance analysis in ^{91}Zr are shown in Fig. 5. Analysis of the 681-eV resonance included only transmission data because of concerns that an error may be introduced in capture

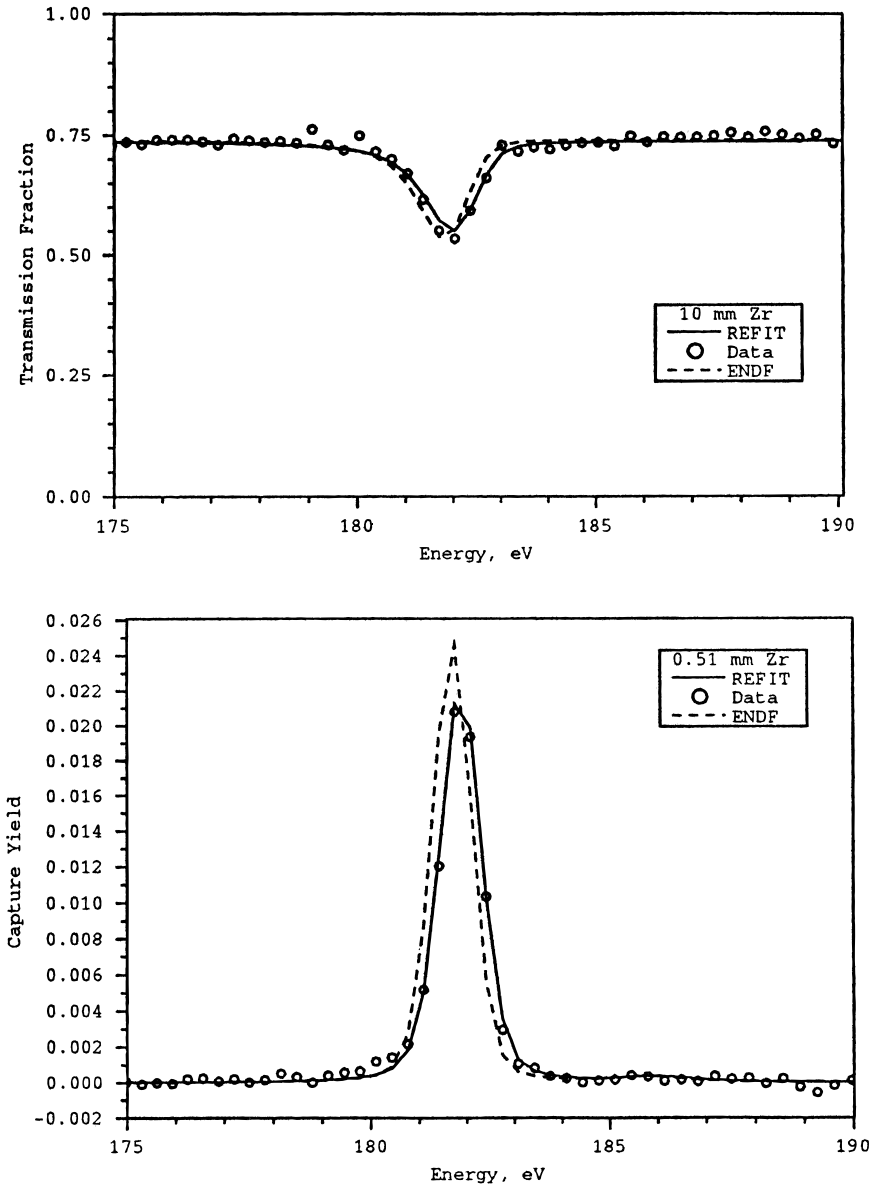

	ENDF J=3	Present Measurements J=4
Energy, (eV)	181.7	181.9 +/- 0.1
Γ_γ (meV)	180	275 +/- 16
Γ_n (meV)	8.61	6.41 +/- 0.08

Fig. 3. 182-eV p-wave resonance in ^{91}Zr.

measurements due to scattering of these higher energy neutrons, which penetrate the annular liner separating the sample from the sodium iodide crystal. This effect, iodine capture of resonance-energy scattered neutrons, is discussed further in the Sec. VI. Wherever capture data were omitted (see Table V), no fit to Γ_γ was made because the transmission data alone are not sensitive to the radiation width. In such cases, Γ_γ values appear in the tables without quoted uncertainties. The fits to the five resonances shown in Figs. 1 through 5 are very good for all samples.

Figure 6 shows the fit to four resonances between 2.1 and 2.5 keV. Neither the 2361- nor the 2383-eV resonances are visible in the present measurements. The

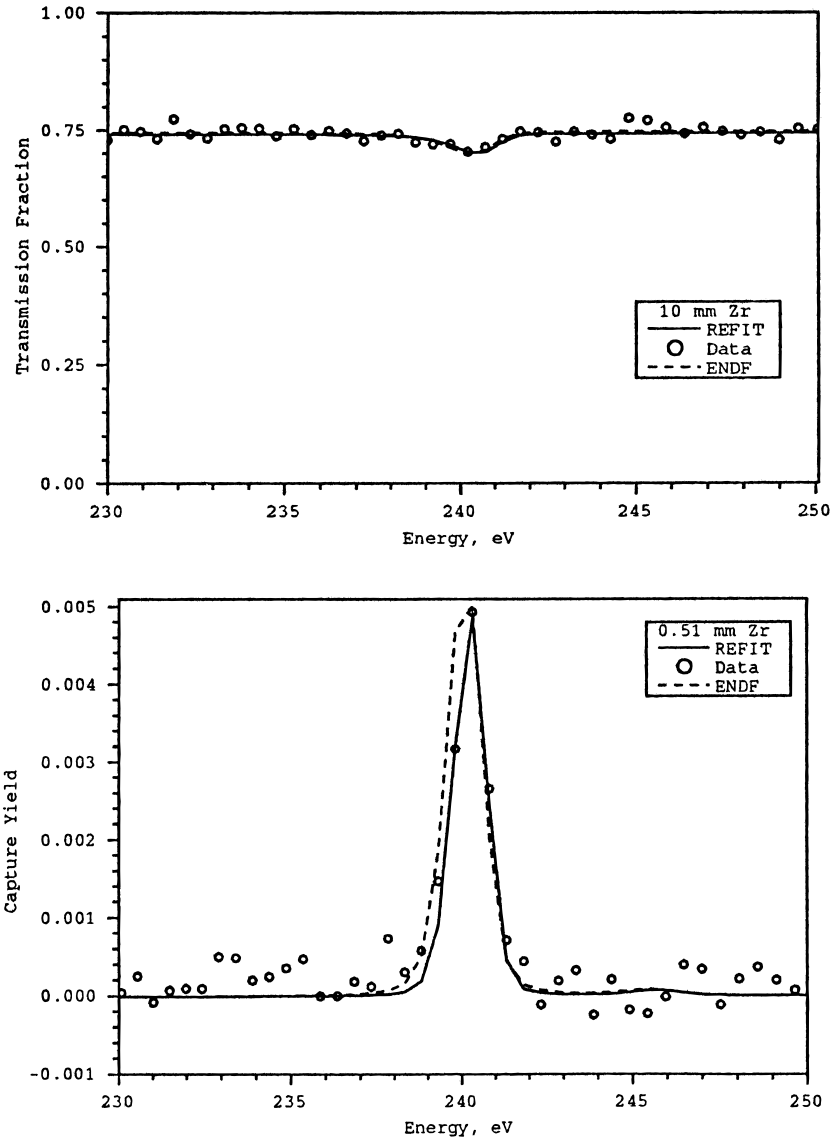

	ENDF	Present Measurements
Energy, (eV)	240.1	240.3 +/- 0.1
Γ_γ (meV)	270	143 +/- 12
Γ_n (meV)	4.32	3.52 +/- 0.12

Fig. 4. 240-eV p-wave $J = 2$ resonance in ^{91}Zr.

ENDF/B-VI evaluation gives $\Gamma_n = 3.5$ eV for the 2361-eV resonance. This Γ_n is much larger than that given by any of the referenced measurements.[10,11,15] Based on the present measurements, this Γ_n is at least one order of magnitude too large.

Figure 7 shows results of two REFIT calculations, not fits, using data from materials that were included as standards in one transmission and one capture measurement. Three uranium samples were included in the first transmission experiment, and one gold sample was included in the capture experiment. The resonance parameters used in the calculated curves are from ENDF and were not varied. The resolution parameters used in the REFIT calculations are the same as those derived for

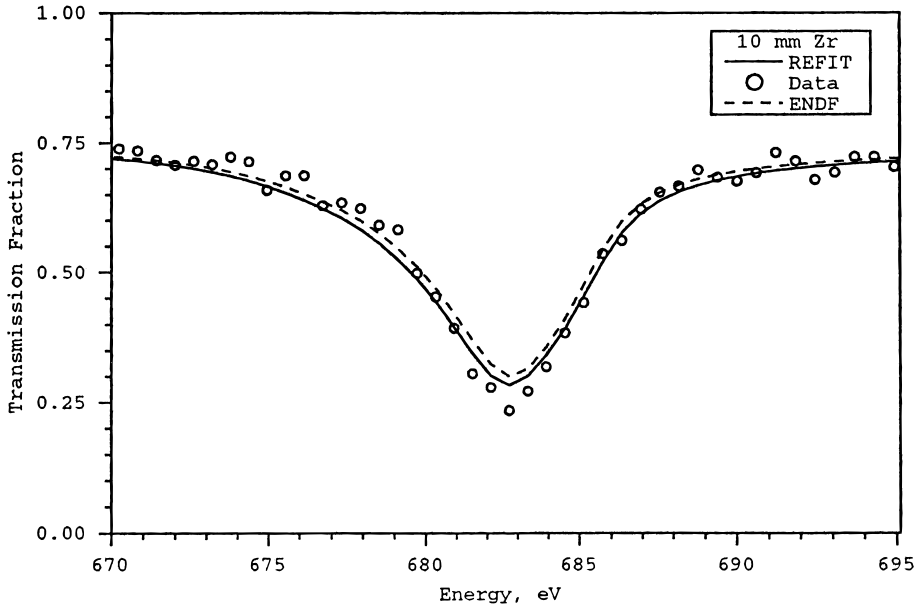

	ENDF	Present Measurements
Energy, (eV)	681.4	681.4 +/- 0.1
Γ_γ (meV)	122	122
Γ_n (meV)	823	922 +/- 8

Fig. 5. 681-eV p-wave $J = 3$ resonance in ^{91}Zr.

zirconium. The agreement of the calculated curves with the experimental data is a confirmation of the adequacy of the resolution parameters used in the present zirconium analysis.

Infinitely dilute capture resonance integrals and thermal capture cross sections from the present measurements are compared with those of ENDF/B-VI in Tables VI and VII. Capture resonance integral (RI) in Tables VI and VII is defined as follows:

$$\mathrm{RI} = \int_{0.5\ \mathrm{eV}}^{\infty} \sigma_c(E)\, dE/E \ , \qquad (2)$$

where $\sigma_C(E)$ is the capture cross section in barns and E is energy in electronvolts.

The uncertainties quoted in the tables are propagated from the uncertainties in Γ_n and Γ_γ given in Table V. Table VI gives the contribution of each resonance to the resonance integral and thermal capture cross section for that isotope. The analyzed resonances contributed only ~10% of the thermal capture cross section. ENDF/B-VI provides Γ_n for the −557-eV ^{91}Zr resonance as 31.32 eV. This is the major contributor to the zirconium thermal capture cross section. Table VII incorporates abundance to yield the contribution of the resonances analyzed to the capture resonance integral and thermal capture cross section for various isotopes as well as for elemental zirconium. The "sum" shown in Table VII reflects only the contributions of the analyzed resonances.

The overall infinitely dilute capture resonance integrals and thermal capture cross sections for ^{91}Zr and elemental zirconium were calculated using ENDF/B-VI parameters for all resonances. The resonance integral was found to be 4.89 b for ^{91}Zr and 0.965 b for elemental zirconium. The thermal capture cross section was found to be 1.19 b for ^{91}Zr and 0.186 b for elemental zirconium.

Table VII data give the differences in infinitely dilute capture resonance integral between the present measurements and ENDF to be +0.118 b for ^{91}Zr and +0.079 b for elemental zirconium. Therefore, the overall infinitely dilute capture resonance integrals for ^{91}Zr and elemental zirconium are 5.01 and 1.04 b, respectively.

Table VII data also give the differences in thermal capture cross section between the present measurements and ENDF to be +0.0035 b for ^{91}Zr and +0.0036 b for elemental zirconium. Therefore, the thermal capture cross sections for ^{91}Zr and elemental zirconium are 1.19 and 0.190 b, respectively.

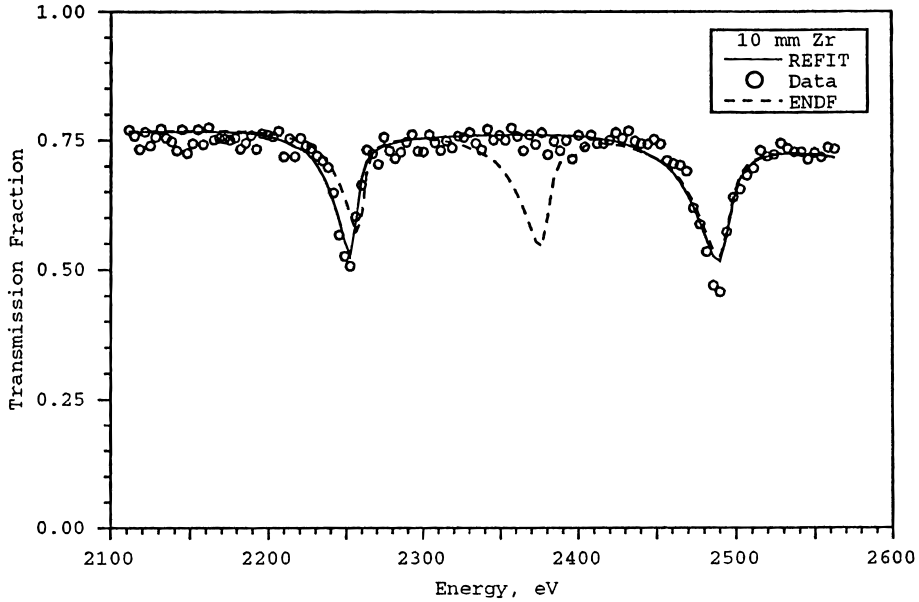

	ENDF	Present Measurements	ENDF	Present Measurements
Energy, (eV)	2243	2239 +/- 1	2361.2	NOT OBSERVED
Γ_γ (meV)	97	97	136	
Γ_n (meV)	1230	1707 +/- 35	3514	
	ENDF	Present Measurements	ENDF	Present Measurements
Energy, (eV)	2474.2	2474 +/- 1	2383.3	NOT OBSERVED
Γ_γ (meV)	140	140	252	
Γ_n (meV)	5784	6284 +/- 107	146	

Fig. 6. 2243-eV s-wave $J = 0.5$ resonance in ^{94}Zr; 2361-eV s-wave $J = 3$ resonance in ^{91}Zr; 2384-eV p-wave $J = 3$ resonance in ^{91}Zr; 2475-eV s-wave $J = 2$ resonance in ^{91}Zr.

VI. DISCUSSION

The present measurements confirm the spin assignments from ENDF/B-VI with the exception of two resonances, 292.5- and 182-eV resonances in ^{91}Zr. The present assignment of $J = 3$ for the 292.5-eV s-wave resonance in ^{91}Zr is especially significant as it clarifies decades of conflict as shown in Table I. The present measurements confirm the $J = 3$ assignment of Salah et al.[8] for this resonance. Figure 2 contrasts the best fits possible with each J value. For the 2.5-mm data shown in the figure, the reduced χ^2 was 1.0 for $J = 3$ and 2.2 for $J = 2$. For the 0.56-mm data shown in the figure, the reduced χ^2 was 1.3 for $J = 3$ and 5.2 for $J = 2$.

A survey of Γ_γ values from the first 21 positive-energy ^{91}Zr $J = 3$ resonances from ENDF/B-VI yielded a mean value of 134 meV with a standard deviation of 12 meV. The standard deviation was calculated from the central values. The concluded 292-eV resonance Γ_γ = 125.9 meV is within one standard deviation of the mean.

A survey of Γ_γ values from the first 14 positive-energy ^{91}Zr $J = 2$ resonances from ENDF/B-VI yielded a mean value of 138 meV with a standard deviation of 29 meV (based on central values). The best fit $J = 2$ Γ_γ = 182.9 meV lies 1.5 standard deviations above the mean.

The doublet near 300 eV is of particular interest, because it contributes ~50% of the resonance integral for zirconium. Resonance parameters for this doublet from various measurements and evaluations are given in Table I. Although the spin assignment for the 292-eV resonance varies, the quantity $2g\Gamma_n$ is nearly equal among ENDF/B-VI, Salah et al., and the present measurements. The quoted uncertainties in the resonance parameters from

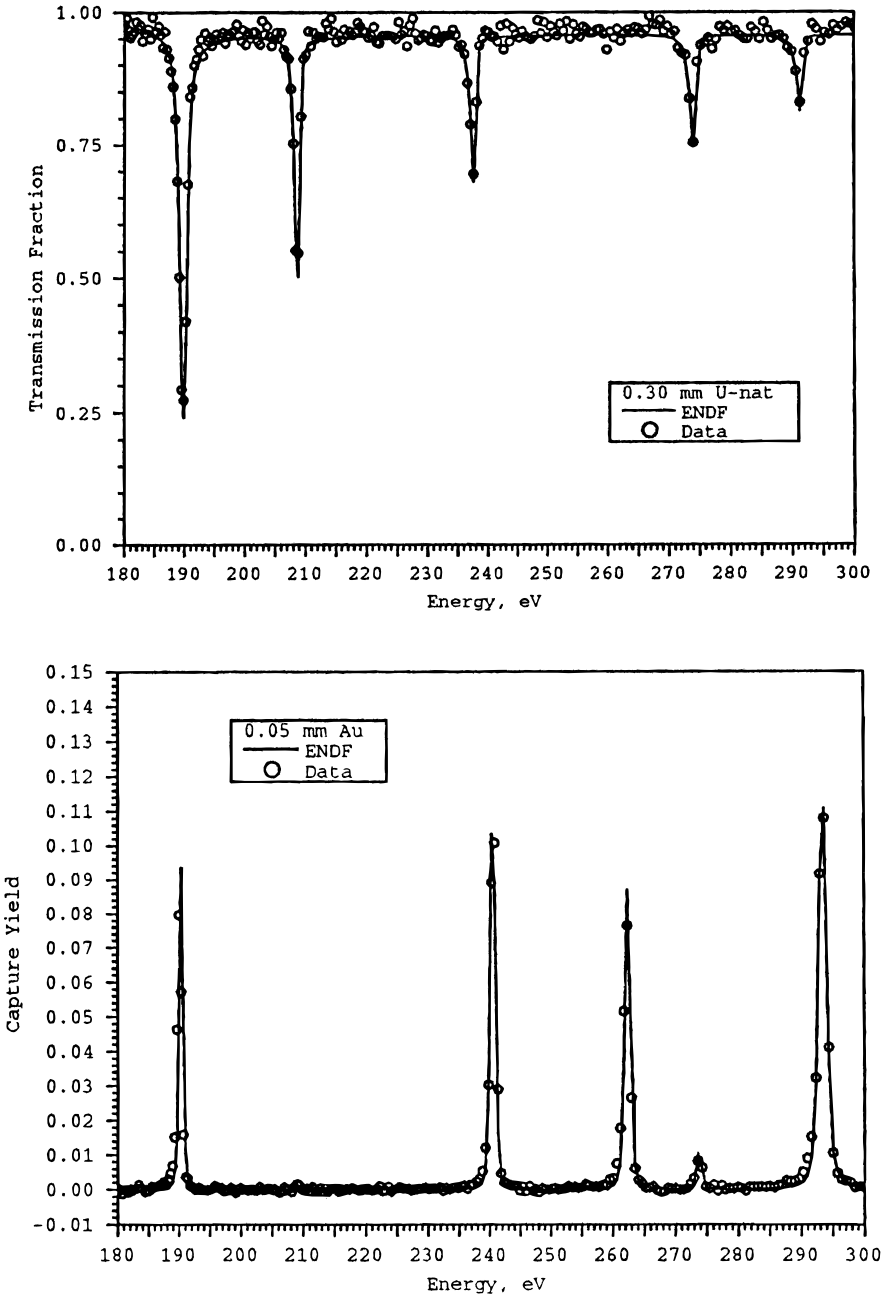

Fig. 7. Confirmation of resolution functions.

the present measurements reflect only the propagated counting statistics from the data. The systematic errors are not included.

The present measurement of resonance parameters for the 292-eV resonance falls within the range of recent measurements as does the neutron width for the 301-eV resonance (see Table I). The 301-eV resonance radiation width is smaller than previously reported. Figure 1 shows that when a larger value (ENDF) of Γ_γ is plotted, the area and width of the resonance in capture are not well represented.

The recommended resonance parameters based on the present measurements yield a reduced χ^2 of 1.2 for the 0.051-mm capture data and a reduced χ^2 of 3.3 for the 0.10-mm capture data. For comparison, the ENDF value of $\Gamma_\gamma = 258$ was fixed, and Γ_n was fitted to capture and transmission data, resulting in $\Gamma_n = 211.6$ meV. The reduced $\chi^2 = 4.8$ for the 0.051-mm capture data, and $\chi^2 = 10.0$ for the 0.10-mm capture data. The Salah et al. value of $\Gamma_\gamma = 285$ was fixed, and Γ_n was fitted to capture and transmission data, resulting in $\Gamma_n = 209.7$ meV. The

TABLE VI

Capture Resonance Integrals and Thermal Capture Cross Sections (0.0253 eV) for ^{91}Zr*

Nominal Resonance Energy (eV)	Infinitely Dilute Capture Resonance Integrals		Thermal Capture Cross Sections	
	ENDF/B-VI	Present Measurements	ENDF/B-VI	Present Measurements
182	0.608	0.595 (0.049)	1.19E-06[a]	1.73E-06[a] (0.10E-06)
240	0.129	0.104 (0.013)	2.40E-07	1.04E-07 (0.09E-07)
292	1.83	3.01 (0.05)	1.03E-01	1.36E-01 (0.02E-01)
301	5.41	4.02 (0.22)	1.24E-05	7.10E-06 (0.36E-06)
681	0.559	0.567 (0.070)	2.03E-02	2.27E-02 (0.28E-02)
2240	0.0748	0.0766 (0.0082)	2.10E-03	2.92E-03 (0.31E-03)
2361	0.0574	0	4.31E-03	0
2383	0.0398	0	3.44E-09	0
2474	0.0390	0.0390 (0.0057)	4.64E-03	5.04E-03 (0.73E-03)

*Units are barns. Uncertainties are based on the uncertainties in Γ_γ and Γ_n shown in Table V. Where no uncertainty is quoted in Table V, Mughabghab, Divadeenam, and Holden[9] values are used. Where Mughabghab, Divadeenam, and Holden[9] have no quoted uncertainty (Γ_γ for 2361-eV resonance) an uncertainty of zero was used.

[a]Read as 1.19×10^{-6}.

TABLE VII

Capture Resonance Integrals and Thermal Capture Cross Sections (0.0253 eV) for Elemental Zirconium*

Zirconium Isotope	Abundance	Infinitely Dilute Capture Resonance Integrals		Thermal Capture Cross Sections	
		ENDF/B-VI	Present Measurements	ENDF/B-VI	Present Measurements
91	0.1122	0.366	0.484 (0.011)	1.48E-02 [a]	1.83E-02 (0.04E-02)
94	0.1738	0.013	0.013 (0.001)	3.64E-04	5.08E-04 (0.53E-04)
96	0.0280	0.152	0.112 (0.006)	3.48E-07	1.99E-07 (0.10E-07)
Sum		0.530	0.609 (0.013)	0.0152	0.0188 (0.0004)

*Units are barns.

[a]Read as 1.48×10^{-2}.

reduced $\chi^2 = 5.7$ for the 0.051-mm capture data, and $\chi^2 = 12.5$ for the 0.10-mm capture data.

A reason for the difference between the current result of Γ_γ for the 301-eV resonance in ^{96}Zr and previous measurements could be a better characterization of our resolution function whose width is comparable to the natural width of the resonance. Our results are based on two independent measurements, transmission and capture, while Salah et al. measured only transmission.

The net effect of the increase in Γ_γ for the 292-eV resonance and decrease in Γ_γ at the 301-eV resonance is a small increase in the resonance integral for zirconium. The overall effect of the present measurements on the zirconium resonance integrals and thermal cross sections is shown in Tables VI and VII. The p-wave resonances contribute significantly to the resonance integral but are far less important in terms of thermal cross section.

Results for the 182-eV p-wave resonance in ^{91}Zr are given in Table V and Fig. 3. The present measurements support the p-wave, $J = 4$ assignment of Brusegan et al.[10] The present neutron width also agrees with Brusegan et al.,[10] and the quantity $2g\Gamma_n$ agrees with ENDF/B-VI within the quoted uncertainties. However, the radiation width was found to be larger than previously reported. Also, the ENDF parameters yield a curve too narrow to fit the capture data and a peak cross section

that is too large (see Fig. 3). Capture is the dominant interaction mechanism in this resonance. Therefore, the area under the resonance in the capture measurement is proportional to Γ_n. The natural width ($\Gamma_n + \Gamma_\gamma$) is extracted from the difference between the observed width and the resolution and Doppler widths. Using the present measurement's resonance parameters from Table V, the ratio of observed-to-natural width is ~4:1. Therefore, the data are not very sensitive to the choice of radiation width. If Γ_γ is fixed to the ENDF value of 180 meV, then the resultant $\Gamma_n = 6.21$ meV with a <5% increase in the goodness of fit reduced χ^2.

Results for the 240-eV p-wave resonance in ^{91}Zr are given in Table V and Fig. 4. A weak resonance is shown by the transmission plot in Fig. 4. The radiation width quoted gave the best simultaneous fit to one transmission and three capture samples. The radiation width is smaller than previously measured. The capture plot in Fig. 4 shows that the ENDF curve is too broad to fit the data, and therefore the REFIT result is a greatly reduced Γ_γ. The 240-eV resonance is similar to the 182-eV resonance in the respect that it is predominantly capture resonance. Using the current measurement's resonance parameters from Table V, the ratio of observed-to-natural width is ~8:1. If Γ_γ is fixed to the ENDF value of 270 meV, then the resultant $\Gamma_n = 3.17$ meV with a <5% increase in the goodness of fit reduced χ^2.

In Table V, the uncertainties (1σ) are given in parentheses next to the data values. Where no parentheses appear in the table for the present measurements, the value was fixed and not fitted. The present measurements' uncertainties are those evaluated by REFIT for the simultaneous capture/transmission analysis. The transmission and capture measurements are independent and complementary methods for determining resonance parameters. All the uncertainties given in Table V are propagated random statistical uncertainties, but do not reflect systematic errors that are common to both capture and transmission measurements. Possible sources of systematic uncertainties include using the same electron accelerator, the same neutron-producing target, the same method for determining flight path length, some of the same zirconium samples, and some of the same data acquisition electronics. These uncertainties, common to both types of experiment, are judged to be insignificant.

Capture data were excluded above the 300-eV doublet (as illustrated in Table V) because of concerns that at this energy the $^{10}B_4C$ inner detector liner admits neutrons into the NaI crystal at a rate of ~7 per 1000 scatters.[24] These neutrons could subsequently be captured in the iodine of the detector crystal and mistakenly counted as a capture in zirconium. This effect is larger with increased neutron energy and for strong scatterers. The estimates of liner penetration of scattered neutrons result from Monte Carlo calculations. The error introduced is magnified when the number of captures is small compared with the number of scatters. For the worst-case scenario, where capture data were included, the effect is <4% in the 301-eV resonance. That is, <4% of the zirconium-measured capture area at 301 eV could be due to scatters in zirconium and subsequent capture in iodine. The effect iodine capture has on extracted resonance parameters is considered to be trivial for the following reasons:

1. For the 301-eV resonance in ^{96}Zr, the increased flight path of a neutron traveling several centimetres after being scattered in a resonance would place the count outside of the measured resonance. Therefore, the area under the resonance would be due only to capture in zirconium.

2. A buildup of background at high energy (>1 keV) beyond that subtracted using the empty sample holder method was observed. If iodine capture appears as an additional background, it would be partially accounted for in the REFIT calculation by fitting the background. As recommended in the REFIT manual, background was fitted for all capture measurements.

3. Test calculations were made for the 681-eV resonance where the iodine capture effect is much greater. Since more liner penetration occurs at higher neutron energies and the scatter-to-capture ratio at 681 eV is roughly double that at 301 eV, as much as 50% of counts measured as captures could be due to scattering (and subsequent capture in iodine). However, whether capture data were included and Γ_γ fitted or capture data was excluded and Γ_γ fixed, the same resonance parameters were extracted.

For these reasons the iodine capture does not significantly affect the current set of resonance parameters. Iodine captures are occurring, but they appear outside of the measured resonance. References to the values of 4% at 301 eV and 50% at 681 eV for these particular zirconium resonances are based on the worst-case assumption. That is, if the scattered neutron penetrates the boron liner, it will be captured in iodine, and its subsequent gamma rays will be detected and scored as a capture.

Results for the 681-eV s-wave resonance in ^{91}Zr are given in Table V and Fig. 5. A neutron width larger than the ENDF value resulted in a somewhat better fit to seven transmission samples.

The fits in the 2.1- to 2.5-keV range are not as good as fits for the lower energy resonances because the measurements were optimized for the 300-eV doublet (see Fig. 6). Resonances in the 2.1- to 2.5-keV range could be better resolved using the RPI LINAC and transmission detector if an experiment were designed for this purpose. The data do not show the presence of either the 2361- or 2383-eV resonance. The 2383-eV resonance is weak, so it is not surprising that it was not seen. However, REFIT calculations show that the 2361-eV resonance would be visible if its Γ_n were even 10% of the ENDF value. Thus, the strength of the 2361-eV resonance in ^{91}Zr has previously been significantly overestimated. The fit to the

2239-eV resonance increases the neutron width substantially over the ENDF value and improves the goodness of fit.

The single set of resonance parameters presented here fit data from multiple sample thicknesses and three independent experiments rather well. Uncertainties are generally smaller than those of Mughabghab, Divadeenam, and Holden.[9] In fact, fits from the thickest samples, 0.51 mm for capture and 10 mm for transmission, as shown in most of the figures are certainly adequate (reduced $\chi^2 = 1.20$ and 1.56, respectively). The fits for thinner samples are generally even better. Also, gold sample data taken in the zirconium capture measurement and broadened with the present capture resolution function show good agreement with known parameters. The same was found when uranium data taken in one of the zirconium transmission experiments were broadened with the present transmission detector resolution function and compared with known resonance parameters (Fig. 7).

VII. CONCLUSIONS

The RPI measurement and analysis of zirconium capture and transmission data at the RPI LINAC has improved the accuracy and understanding of the neutron cross-section parameters. The present results were based on a simultaneous analysis using all reliable data sets for each resonance as shown in Table V. Separate resolution functions for transmission and capture were established using zirconium data and confirmed using uranium and gold data.

The results of the REFIT calculations show good fits to experiment when plotted against the data sets. The most significant findings are as follows:

1. confirmation of Salah et al.[8] values for J and Γ_γ for the 292-eV resonance in ^{91}Zr
2. significantly smaller Γ_γ for the 301-eV resonance in ^{96}Zr
3. significantly smaller Γ_γ for the 240-eV resonance in ^{91}Zr
4. significantly larger Γ_γ for the 182-eV resonance in ^{91}Zr
5. absence of evidence of either the 2361- or 2383-eV resonances in ^{91}Zr. The Γ_n for the 2361-eV resonance is at least an order of magnitude smaller than that given by ENDF/B-VI (Ref. 7).

The statistical uncertainties were propagated through the REFIT code and are generally smaller than those reported by Mughabghab, Divadeenam, and Holden.[9] Although these uncertainties do not contain an allowance for systematic errors, the contributions from such errors are expected to be small because the present REFIT analysis included both capture and transmission measurements, which are independent methods.

The effect of the present results on the infinitely dilute capture resonance integral for elemental zirconium is a 79-mb (8%) increase to 1.04 b. The effect of the present results on the thermal capture cross section for elemental zirconium is a 3.6-mb (2%) increase to 0.190 b. These results indicate a significant increase in zirconium capture resonance integral, and, while the capture resonance integral is relatively small, zirconium is present in large quantities in nuclear reactors.

REFERENCES

1. R. E. SLOVACEK, R. C. BLOCK, Y. DANON, C. WERNER, G.-U. YOUK, J. A. BURKE, N. J. DRINDAK, F. FEINER, J. A. HELM, and K. W. SEEMANN, "Neutron Cross Section Measurements at the Rensselaer LINAC," *Proc. Topl. Mtg. Advances in Reactor Physics*, April 11–15, 1994, Knoxville, Tennessee, Vol. II, p. 193, American Nuclear Society (1994).

2. N. J. DRINDAK, F. FEINER, K. J. SEEMANN, and R. E. SLOVACEK, "A Multiplicity Detector for Accurate Low-Energy Neutron Capture Measurements," *Proc. Int. Conf. Nuclear Data for Science and Technology*, May 30–June 3, 1998, Mito, Japan, p. 383.

3. R. C. BLOCK, Y. DANON, R. E. SLOVACEK, C. J. WERNER, G. YOUK, J. A. BURKE, N. J. DRINDAK, F. FEINER, J. A. HELM, J. C. SAYRES, and K. W. SEEMANN, "Neutron Time-of-Flight Measurements at the Rensselaer Linac," *Proc. Int. Conf. Nuclear Data for Science and Technology*, May 9–13, 1994, Gatlinburg, Tennessee, Vol. 1, p. 81, American Nuclear Society (1994).

4. M. C. MOXON, "REFIT, A Least Square Fitting Program for Resonance Analysis of Neutron Transmission and Capture Data," AEA-InTec-0470 (1991).

5. Y. DANON, C. J. WERNER, G. YOUK, R. C. BLOCK, R. E. SLOVACEK, N. C. FRANCIS, J. A. BURKE, N. J. DRINDAK, F. FEINER, and J. A. HELM "Neutron Total Cross-Section Measurements and Resonance Parameter Analysis of Holmium, Thulium, and Erbium from 0.001 to 20 eV," *Nucl. Sci. Eng.*, **128**, 61 (1998).

6. C. J. WERNER, "Total, Capture and Self-Indication Neutron Cross Section Measurements of Tungsten," PhD Thesis, Rensselaer Polytechnic Institute (1999).

7. "ENDF/B-VI Nuclear Cross Sections," Brookhaven National Nuclear Data Center (on-line data service updated to Mar. 1997).

8. M. M. SALAH, J. A. HARVEY, N. W. HILL, A. Z. HUSSEIN, and F. G. PEREY, "Accurate Determination of the Parameters of the 292.4-eV Resonance of ^{91}Zr and the 301.1-eV

Resonance of ^{96}Zr," *Proc. Int. Conf. Nuclear Data for Basic and Applied Science*, Santa Fe, New Mexico, 1985, p. 593.

9. S. F. MUGHABGHAB, M. DIVADEENAM, and N. E. HOLDEN, *Neutron Cross Sections*, Vol. 1, Part A, Academic Press, New York (1981).

10. A. BRUSEGAN, F. CORVI, G. ROHR, C. COCEVA, P. GIACOBBE, and M. MAGNANI, "Neutron Resonance Parameters of ^{91}Zr," *Proc. Int. Conf. Neutron Physics and Other Applied Purposes*, Harwell, United Kingdom, September 25–29, 1978, p. 706, OECD Publication.

11. A. R. DE L. MUSGROVE, J. W. BOLDEMAN, B. J. ALLEN, J. A. HARVEY, and R. L. MACKLIN, "High Resolution Neutron Transmission and Capture for ^{91}Zr," *Aust. J. Phys.*, **30**, 391 (1977).

12. R. L. MACKLIN, J. A. HARVEY, J. HALPERIN, and N. W. HILL, "The 292.4-eV Neutron Resonance Parameters of Zirconium-91," *Nucl. Sci. Eng.*, **62**, 174 (1977).

13. S. F. MUGHABGHAB and D. I. GARBER, "Neutron Cross Sections," Vol. I, 3rd ed., BNL-325, Brookhaven National Laboratory (1973).

14. K. A. R. RIMAWI, "s-Wave and p-Wave Resonance Neutron Capture in ^{91}Zr, ^{93}Nb, and ^{103}Rh," PhD Thesis, State University of New York at Albany (1969).

15. Z. M. BARTOLOME, R. W. HOCKENBURY, W. R. MOYER, J. R. TATARCZUK, and R. C. BLOCK, "Neutron Radiative Capture and Transmission Measurements of W and Zr Isotopes in the keV Region," *Nucl. Sci. Eng.*, **37**, 137 (1969).

16. J. MORGENSTERN, R. N. ALVES, J. JULIEN, and C. SAMOUR, "Parametres Des Resonances et Fonctions Densites S_0 et S_1 pour Cl, ^{51}V, ^{89}Y, Zr, La, ^{141}Pr et ^{209}Bi," *Nucl. Phys.*, **A123**, 561 (1969).

17. W. M. LOPEZ, F. H. FROHNER, S. J. FRIESENHAN, and A. D. CARLSON, "Cross Section Measurements of Zirconium," *Proc. Conf. Neutron Cross Sections and Technology*, Washington, D.C., March 4–7, 1968, National Bureau of Standards Special Publication, Vol. 299, p. 857 (1968).

18. M. D. GOLDBERG, S. F. MUGHABGHAB, B. A. MAGURNO, and V. M. MAY, "Neutron Cross Sections," Vol. IIA, 2nd ed., BNL-325, Suppl. 2, Brookhaven National Laboratory (1966).

19. B. E. MORETTI, "Molybdenum Neutron Transmission Measurements and the Development of an Enhanced Resolution Neutron Target," PhD Thesis, Rensselaer Polytechnic Institute (1996).

20. Y. DANON, "Design and Construction of the RPI Enhanced Thermal Neutron Target and Thermal Cross Section Measurements of Rare Earth Isotopes," PhD Thesis, Rensselaer Polytechnic Institute (1993).

21. G. LEINWEBER, "Calculations of Multiplicity and Efficiency from Neutron Capture in the RPI Multiplicity Detector," PhD Thesis, Rensselaer Polytechnic Institute (1994).

22. D. K. OLSEN, G. DE SAUSSURE, R. B. PEREZ, F. C. DIFILIPPO, R. W. INGLE, and H. WEAVER, "Measurement and Resonance Analysis of Neutron Transmission Through Uranium-238," *Nucl. Sci. Eng.*, **69**, 202 (1979).

23. D. B. SYME, "The Black and White-Filter Method for Background Determination in Neutron Time-of-Flight Spectrometry," *Nucl. Instrum. Methods*, **198**, 357 (1982).

24. G. LEINWEBER, "Analysis of Moxon-Rae and Multiplicity Detectors Using Monte Carlo Techniques," MS Thesis, Rensselaer Polytechnic Institute (1989).